

Manufacturing 3-D Lithium-ion Batteries with Interpenetrating Lattice Electrodes

Thesis by

Nathan Zou

Submitted to the Department of Chemistry and Chemical Engineering
In Partial Fulfillment of the Requirements for the Degree of
Bachelor of Science in Chemical Engineering

The logo for the California Institute of Technology (Caltech), featuring the word "Caltech" in a bold, orange, sans-serif font.

CALIFORNIA INSTITUTE OF TECHNOLOGY
Pasadena, California

June 2023

ACKNOWLEDGEMENTS

My journey to discover my passion for energy storage research has been one of the best experiences of my life so far. There are so many people I am extremely thankful for who have provided the support and guidance for me to pursue my interests and make small but important discoveries. I would like to begin by thanking Dr. Julia Greer for providing such a welcoming and nurturing culture within her lab. Going to group meetings really captured my interests in the Greer Group mission for advancing the field of architected materials, spurring my decision in joining the lab and making contributions. Additionally, I would like to thank my graduate mentors Yuchun Sun and Yingjin Wang, who have always been there to guide me throughout my research process and challenging me to think outside the box in the laboratory setting. The direction in which my project was heading treads through unexplored areas of research, and I knew there were going to be many challenges that will require extensive troubleshooting and creative thinking. Dr. Greer, Yuchun, and Yingjin have been so supportive in my research endeavors and were always there to provide me unique insight when I faced significant roadblocks. Without their guidance, my progress on this project would not have been possible. I would also like to thank lab members Fernando Villafuerte, Seneca Velling, Sammy Shanker, and Andrew Friedman for their help and insight ever since I joined the Greer lab.

Additionally, I would like to thank my previous research mentors for helping steer me towards finding my passion for a topic in STEM such that I can invest my career towards its advancement. Dr. Nathan Lewis, Dr. Yuk Yung, Dr. Richard Flagan, Dr. John Seinfeld, Dr. Katie Hamann, and Dr. Yuan Wang have all provided me the necessary guidance throughout this process. I will always appreciate the valuable experience, science, and inspiration they have shared with me. I would like to thank my professor and option advisor, Dr. Mike Vicic, for

always trying to improve every aspect of Caltech's chemical engineering program and for always being there for me when I faced challenges in courses or needed guidance in my career pursuits.

As a student-athlete pursuing one of the busiest options at Caltech and concurrently working in a research lab, I am profoundly grateful for the unwavering support of my friends, who consistently instilled their belief in me during challenging times. I would like to specifically thank Hernan Caceres, Joon Young Park, Kyle Reese, Carl Cheng, Andrew Pasco, Josh Finnerty, Daniel Li, Anas Zouhar, Jack Pierson, Ben Juarez, Kyle McGraw, Eli Seiner, Shelby Scott, Nicole Lee, Sydney Serratos, Georgia Malueg, and the tennis team (Rishi Gundakaram, John Kim, Kyle McCandless, Daniel Wen, Victor Li, Andrei Staicu, Ishaan Kannan, Bharathan Sundar, Aditya Srinivasan, Andrew Zabelo, Jonathan Lin) for creating a community that I am so lucky to belong in at Caltech. All of these people have played a crucial role in my personal growth and have helped make my undergraduate student experience feel complete.

Lastly, I would like to express how grateful I am to my parents for their persistent support, which has been a constant source of inspiration, strength, and encouragement throughout my life. To Jon Ransom and Ying Ding, your unwavering dedication, countless hours of effort, and selfless sacrifices spent on raising me has paved the path for me to excel here at Caltech today. No matter where I go in life, my biggest hope is that I can keep making the both of you proud.

ABSTRACT

3-D lithium-ion batteries have been proven to exhibit a higher energy density while minimizing power loss compared to the standard, layer-by-layer constructed 2-D lithium-ion batteries. This thesis explores the implementation of additive manufacturing in the process of constructing the proposed 3-D battery due to its capability of architecting materials with high accuracy and tunability. A 3-D lithium-ion battery backbone was created using a 2-step process, in which the first step 3-D printed the overall structure as a polymer, and the second step sputtered gold onto the polymer for conductive properties. The 3-D printed battery backbone consisted of two interpenetrating lattices made of post-cured PR48 resin that would serve as the anode and cathode, while the electrolyte would fill the space between the two electrodes. During the sputtering process, the polymer structure was rotated 6 times to guarantee that the sputtering will be conformal throughout the lattice. Electrodeposition was used to generate a LiCoO_2 anode and a Li cathode. The electrodeposition of the lithium cobalt oxide cathode onto the lattice structure was proven to be unsuccessful due to the low thermal stability and high reactivity of the 3-D printed polymer when submerged into the electrolyte, consisting of KOH at 260 °C. Results indicate that the uniform electrodeposition of the lithium anode onto the lattice structure was successful using a 1s on, 1s off pulse current for a 60-minute duration. Using a titanium and gold layer proved to increase the uniformity of the coating. However, due to the failure of the lithium cobalt oxide electrodeposition, a different backbone structure may need to be considered. Having two separate structures serving as the anode and cathode (and later combining them into one structure) as opposed to both electrodes being on one structure may be beneficial. This allows for the cathode to be altered without altering both electrodes, allowing more flexibility to coat the structure with lithium cobalt oxide.

TABLE OF CONTENTS

ACKNOWLEDGEMENTS.....	ii
ABSTRACT.....	iv
LIST OF FIGURES, EQUATIONS, AND TABLES.....	vi
INTRODUCTION	1
The Importance of Energy Storage	1
Why 3D Batteries?	2
Additive Manufacturing and Vat Polymerization	3
Proposed Interpenetrating Lattices 3-D Battery Structure	6
Manufacturing Procedure Outline	7
Analysis of Electrodes and Battery Testing	9
FABRICATION OF 3-D LI-ION BATTERY.....	11
3-D Printing of Lattice Backbone	11
Coating of Lattice Backbone with Gold.....	11
Electrodeposition of Lithium Cobalt Oxide (LCO) Cathode	12
Thermal Analysis of Polymer Backbone under LCO Electrodeposition Conditions.....	13
Exploration of Ceramic Resins	15
Using Ceramic Resin for Battery Backbone Structure.....	16
Electrodeposition of Lithium Anode.....	19
SEM Analysis of Plated Lithium	22
Addition of Titanium and Gold Layer to Pyrolyzed Carbon Micro-Lattice	23
Lithium Electrochemistry Setup Optimization	24
Utilization of Pulse Current in Lithium Electrodeposition	28
CONCLUSION.....	31
Project Summary	31
Future Work	32
REFERENCES	34

LIST OF FIGURES, EQUATIONS, AND TABLES

Figure 1: Examples of Possible 3-D Battery Designs.....	3
Figure 2: Schematic of Vat Polymerization Stereolithography	4
Figure 3: Tradeoff Between Energy Density and Power Density.....	5
Figure 4: Image of the Interpenetrating Lattices Backbone.....	6
Figure 5: Gold-coated Structure with Electroplated Nickel on One Lattice.....	8
Figure 6: Gold-coated PR48 Stick Samples.....	13
Figure 7: Steps for Additively Manufacturing Ceramic Materials	15
Figure 8: Relationship Between Cure Time and Layer Thickness	17
Figure 9: Troubleshooting the Overexposed First Layers of the Lattice	18
Figure 10: Printed Lithium Micro-lattices	19
Figure 11: Electrodeposition Setup.....	21
Figure 12: Chronopotentiometry Data for Electroplating.....	22
Figure 13: SEM Images of Dendritic Lithium Growth.....	23
Figure 14: SEM Images of Electroplated Lithium on Pyrolyzed Carbon vs Gold	24
Figure 15: Relationship Between Current Density and Electrode Separation.....	25
Figure 16: Fabrication Process of New Electrodeposition Setup	26
Figure 17: SEM Image of Entire Micro-lattice with New Electrodeposition Setup.....	26
Figure 18: SEM Images of Electroplated Lithium at Various Durations	27
Figure 19: SEM Images of Sample Following 60-minute Pulse Current	29
 Equation 1: Relationship Between Diffusion Time (t) and Diffusion Length (x)	 5
 Table 1: Relationship Between Post-cure Time and Mass	 14

INTRODUCTION

The Importance of Energy Storage

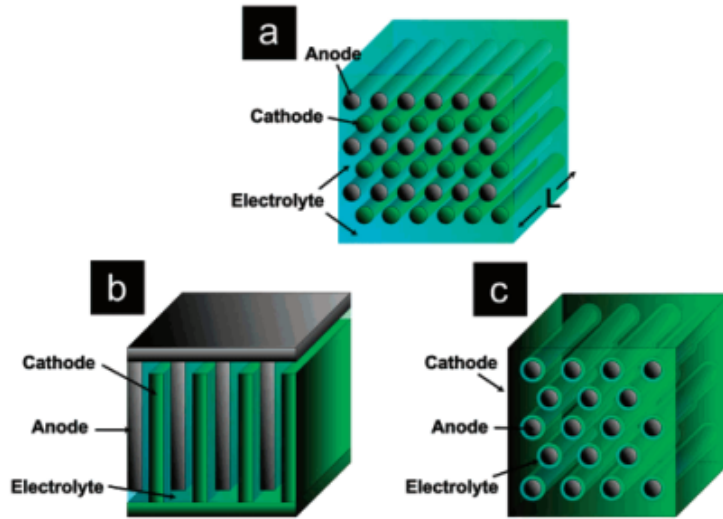
The continuous growth of electric vehicles and sustainable energy sources spur the global demand for improved energy storage devices to supply power for longer durations. Major renewable energy sources such as wind and solar power are limited due to the energy's intermittency; the sun and wind are not always available when needed. The limited amount of available sunlight is further exacerbated at higher latitudes, where there is even less light that reaches the surface due to the obliquity of the Earth. Wind's intermittency is more significant, harder to predict, and generally only a constant supply of energy in coastal and offshore regions¹. By achieving higher energy density to increase energy storage as well as minimizing energy loss, the sun and wind's intermittency would no longer remain problems, since batteries can provide stored energy for when the intermittent energy sources are unavailable.

Additionally, improvements in energy storage techniques will facilitate the expanded integration of batteries in various modes of transportation. This advancement will yield a significant departure from the prevalent reliance on natural gas for powering cars, buses, trains, and even airplanes, thus yielding a significant reduction in global carbon emissions. The combination of increased reliance on renewable energy sources and reducing gas-powered modes of transportation will play a tremendous role in reducing the human carbon footprint on the earth. However, improving battery storage, energy density, and cyclability are still challenges waiting to be solved, which is why batteries remain as one of the major limiting steps in the transition towards a more sustainable world.

Why 3-D Batteries?

The term "3-D batteries" does not refer to the physical dimensions, or appearance, of the battery itself. Instead, it denotes the intricate mechanisms through which ions are transported between electrodes within the battery. The idea of 3-dimensional batteries has been circulating within the scientific community in the past couple decades soon after the major advancements of the standard 2-D lithium-ion battery². Although the lithium-ion battery proved to be extremely advantageous performance wise compared to previous batteries, the layer-by-layer construction of the cells in the standard 2-D batteries limits the maximum power and energy density that could be achieved. This is because the constructed orientation forces the lithium ions to travel perpendicularly between the electrodes, restricting the energy to be proportional to the cell area. In other words, larger layers allow more lithium ions to freely diffuse between electrodes. This directly limits the energy density, or power supplied per area, of the battery. Energy density can be increased by making the electrode layers thicker, but this will in turn reduce the power of the battery due by increasing the lithium-ion diffusion length, and hence the diffusion time³. For these reasons, 2-D lithium-ion batteries are approaching their theoretical limits, as recognized by the scientific community.

However, by incorporating multiple electrodes arranged in intricate geometries enabling nonplanar diffusion of lithium ions, the energy and power tradeoff of the battery can be eliminated. This is because the new arrangements, as shown in Figure 1, allow for a greater electrode surface area per area of the cell, whereas the electrode surface area is equal to that of the cell in the 2-D arrangement. At the same time, both 2-D and 3-D electrode arrangements yield comparable power output. This is because advancements in the field of 3-dimensionally architected materials allows for the maintenance of the small lithium-ion transport distances.

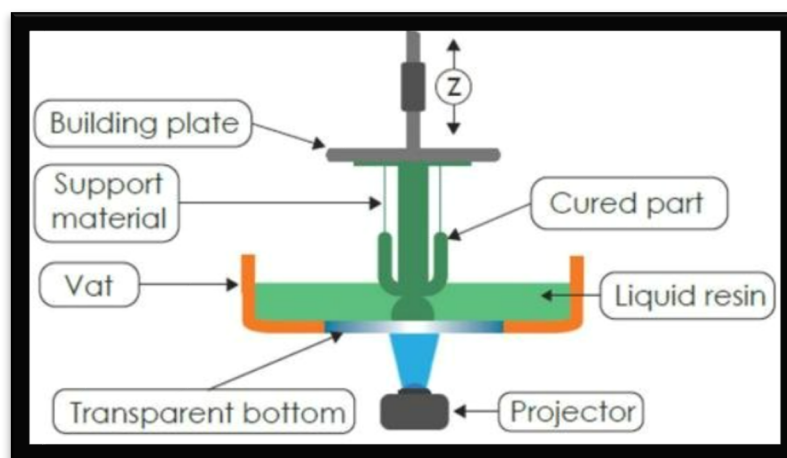


“**Figure 1:** Examples of Possible 3-D Battery Designs: Figure “a” represents an array of cylindrical cathodes and anodes. Figure “b” represents an array of cathodes and anodes as plates. Figure “c” represents an array of cylindrical cathodes, surrounded by a thin layer of electrolyte, with the remaining volume acting as the anode².”

Additive Manufacturing and Vat Photopolymerization

Additive manufacturing is a method of building structures in a layer-by-layer fashion. The process begins with the construction of a 3-dimensional computer-aided design using software such as SolidWorks, AutoCAD, and more. Once the 3-dimensional design is created, it is then uploaded to a 3-D printer, which creates the physical object of the design. 3-D printers are powerful tools that may create objects out of many different materials, including polymers, ceramics, and even metals. Resultant structures can be highly tunable in morphology and are capable of having precise resolution to the micron-scale. Due to this, structures can be architected to have highly advanced functionalities for the fields that they are being applied to. Additionally, little to no waste is produced, which is why additive manufacturing is an extremely efficient and sustainable technology. The ability to accurately create complex, 3-dimensional structures such as lattices and honeycombs at high resolutions makes additive manufacturing a highly promising method for the construction of 3-dimensional batteries.

Vat photopolymerization is a type of additive manufacturing technology that produces 3-D structures by using a highly accurate ultraviolet laser to polymerize a liquid resin. The resin consists of a liquid photopolymer that cures, or hardens, when exposed to UV light. For this thesis, stereolithography, a type of vat polymerization, will be used to manufacture the backbone of the 3-D lithium-ion battery. The stereolithography technique incorporates 3-D printer consisting of a flat metal build head submerged in a vat containing the liquid photopolymer resin and is pressed flat against a UV transparent window. A CAD design that splits the desired structure into thin layers is inputted into the printer. Then, a very focused UV laser is subjected to the vat through the transparent window, where the laser cures the resin into a polymer via a process known as free radical polymerization. Only the resin that comes into contact with the focused UV laser becomes polymerized. The first layer of resin gets cured onto the build head, and the head will slowly move up layer by layer as more resin gets cured, ultimately forming the desired product. Once the desired product is detached from the build head, it may be post-cured with UV radiation to further strengthen their structural and mechanical properties.



“Figure 2: Schematic of Vat Polymerization Stereolithography: The figure above depicts the key features of a stereolithography 3-D printer.”

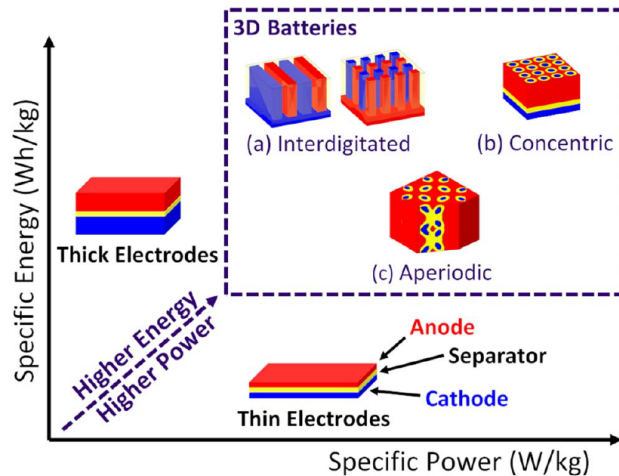
The 3-D battery electrodes will be constructed via additive manufacturing. Additive manufacturing, or 3D printing, is capable of accurately producing highly complex 3-dimensional structures spanning resolutions between microns and centimeters. Due to this, 3D printed electrodes are capable of having even smaller feature sizes than those of standard 2D electrodes. This implies that lithium-ion diffusion length between electrodes can be smaller for 3D batteries. Diffusion time is directly proportional to the square of diffusion length, by the equation shown below. With a lower lithium diffusion time, the battery performs more optimally³. Therefore, a high power-dense battery can be obtained without the cost of decreasing energy density, as aforementioned, with a 3-D electrode arrangement.

$$\boxed{\mathbf{a}} \quad t = \frac{x^2}{D_{eff}}$$

$$\boxed{\mathbf{b}} \quad D_{eff} = D_0 \frac{\epsilon}{\tau}$$

$$\boxed{\mathbf{c}} \quad \tau = \epsilon^{-0.5}$$

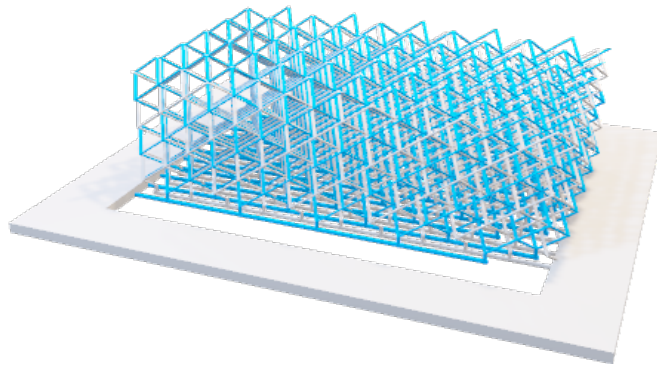
“**Equation 1:** Relationship Between Diffusion Time (t) and Diffusion Length (x): D_{eff} represents the effective diffusivity, which is a function of the intrinsic diffusivity (D_0), electrode porosity (ϵ), and the tortuosity of the porous electrode (τ). The main takeaway is that t and x^2 are directly related².”



“**Figure 3:** Tradeoff Between Energy Density and Power Density: The figure above depicts the tradeoff between energy density and power output of the standard 2-D battery. Increasing the surface area of the electrodes per area of the cell while maintaining the short distance between electrodes, as seen in the 3-D battery geometries, will break this tradeoff⁴.”

Proposed Interpenetrating Lattices 3-D Battery Structure

With the development of a 3-dimensional battery in mind, the proposed structure that this project seeks to develop will first consist of 2 interpenetrating polymer lattices that will serve as backbones for the two electrodes. Previous 3-D battery architectures explored, such as those in Figure 1, have proven to be difficult to fabricate⁴. The interpenetrating lattices backbone can be easily created using a 3-D printing technique. Another motivation for designing a polymer lattice to serve as the backbone of the 3-D battery is the flexibility to design and adjust the geometry of electrodes at different length scales in the 3-D lithium-ion battery. This is important because the geometry of the distributed electrodes in the cell affects the diffusion of lithium ions, and thus the battery current and cycling. By selectively designing the backbone, ion and electron transport can be optimized enhance battery performance⁵. Once the backbone was printed, a gold sputtering coating will be applied to make the backbone electrically conductive so that the anode and cathode can then be electroplated.



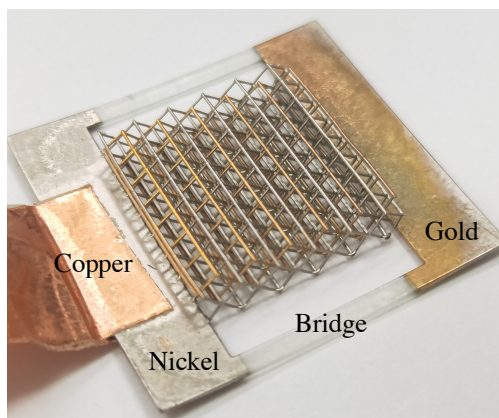
“Figure 4: Image of the Interpenetrating Lattices Backbone: The images above depict the backbone of the 3-D battery for this project. It consists of 2 interpenetrating lattices (serving as the anode and cathode), that do not come into contact with each other. The material used to print this backbone is PR48, a resin that photopolymerizes upon exposure to light.”

Manufacturing Procedure Outline

The project will begin with the synthesis of the backbone of the 3-dimensional battery, as shown in Figure 4. This structure will be created using a 3-D printing technique from the Ember Stereolithography 3D Printer, which prints the structure via the vat photopolymerization process. Structures printed using the Ember printer can have feature sizes as low as 25 microns. A laser of wavelength 405 nm was applied to a resin, hardening the resin layer by layer by a free radical polymerization reaction to form the 3D printed model. The resin will be polymerized onto a build head, which moves up as each layer of polymer gets printed until the product is complete. The laser applies the shape of an object to the surface of the photopolymer container within the printer, which determines the shape of each printed layer. PR48, the standard prototyping resin for every Ember 3D printer, was the chosen photopolymer for the backbone. The overall backbone will have a length of 33 millimeters, a width of 27 millimeters, and a height of 18 millimeters. The electrode beam size will be 0.2 in diameter, and the beams will be spaced approximately 0.9 mm apart.

Once the backbone is printed in the Ember printer, the two bridges of the backbone are covered before gold is sputtered onto the lattice. This is done to keep the two lattices separated from each other (as anode and cathode) via the polymer insulation. By doing this, we will be able to electrodeposit the anode and cathode separately onto each lattice. If the lattices were not conductively separated, the anode and cathode materials would be plated onto the entire structure instead of onto one of the lattices. Another reason that electrodeposition was the chosen method for creating the anode and cathode for our battery is because this method is capable of loading predetermined quantities of the necessary materials onto the lattices. This is important so that the transport of electrons and ions inside the battery can later be quantified. As a proof of concept,

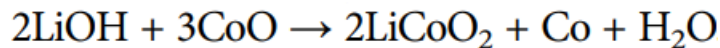
nickel was successfully electrodeposited onto one of the lattices of the proposed structure under ambient air and room temperature conditions (shown in Figure 5).



“Figure 5: Gold-coated Structure with Electroplated Nickel on One Lattice: Nickel was electroplated onto one of the lattices at room temperature. Nickel (silver color) can be seen on one of the lattices and on the left side of the structure, which was connected to the Potentiostat by the conductive copper tape. Because the bridges were kept nonconductive, the right side of the structure—on which the other lattice is connected to—was not plated with nickel.” Image provided by Yingjin Wang.

Lithium metal is chosen as the anode because it has a high oxidation potential (as a small alkali metal), low charge potential, high capacity, and can be electrodeposited at room temperature³. Additionally, as an alkali metal, lithium is known for readily donating its singular valence electron. As a result, lithium anodes contribute to a relatively high voltage batteries compared to other metals, which is highly important for substantial energy storage. The cathode usually consists of a lithium transition metal oxide (LTMO); for this project, lithium cobalt oxide is chosen because it can be conformally electroplated (compared to other LTMOs) on a conducting surface with a selective crystal orientation and allows the resultant battery to deliver a high rate of discharge⁵. One major potential problem to be faced in this project is the high temperature required for the electrodeposition of LiCoO_2 (260 °C). This temperature is necessary because the electrodeposition is based off of a procedure from Zhang et al., comprising of a

solution of LiOH, KOH, and CoO⁶. In this electrodeposition, the following reaction will occur when a voltage is applied:



KOH, a strong base, is the chosen solvent due to its ability to dissolve cobalt but requires a temperature of 260 °C to reach a molten state. Nevertheless, this temperature is significantly lower than those required to synthesize lithium transition metal oxides (700-1000 °C), which are known to be universally utilized cathode materials. Still, the relatively high temperature of the electrodeposition gives rise to a potential issue of electroplating LiCoO₂ without damaging the polymer lattice backbone; if a clear solution cannot be found, alternative strategies must be analyzed, such as the use of a less reactive metal coating, a higher temperature-withstanding backbone material, or an alternative cathode material.

Analysis of Electrodes and Battery Testing

Focused-ion beam scanning electron microscopy (FIB-SEM) will be used to characterize the thickness of electrodeposited materials so that the electrodeposition conditions can be optimized. Once the lattices are electrodeposited with the desired thickness, a gel polymer electrolyte resin will fill the space between the two lattices. Thermal polymerization will be used to solidify the resin that fills the lattice to complete the battery.

Following the manufacturing process, the battery will be analyzed via cycling to determine its capacity and coulomb efficiency. The energy density of the battery will be calculated, knowing the density of the PR48 resin used to form the backbone, the amount of gold sputtered onto the lattices, and the amount of active material (lithium cobalt oxide and lithium) electrodeposited on the gold. The mass ratio between the active materials (anode and cathode

material mass) and current collectors (backbone and gold) will be calculated and compared to commercial lithium-ion batteries to determine the effectiveness of the battery created in this project, and to see which aspects of the design can be improved.

FABRICATION OF 3-D LI-ION BATTERY

3-D Printing of Lattice Backbone

PR48 was poured into the Ember 3D printing tray. Then, the print file of the lattice backbone structure was uploaded to the printer, and the build head was calibrated. This was followed by a successful printing of the backbone. The duration of printing depended on the cure time for the resin and the size of the printed structure, which could be manually adjusted. Print durations ranged from 40-60 minutes. Curing refers to the strengthening of the polymer material, which is directly related to duration of exposure to the laser. One of the significant challenges during the backbone printing process was the removal of the printed sample from the printer build head. A laboratory razor blade was used to manually peel the sample from the build head. At this point, the sample is not fully cured, so the material is not extremely durable. If not careful, the rectangular base would crack during the peeling process, which made the backbone ineffective. Once removed, the sample was placed under strong a broad band, UV light for 15 minutes to post cure to complete the photopolymerization process.

Coating Lattice Backbone with Gold

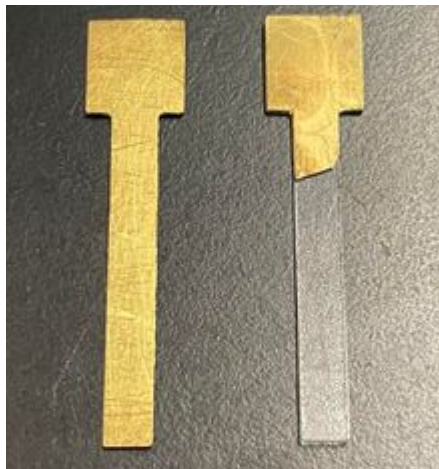
The photopolymerized backbone was loaded into a glovebox and placed into the sputter coating system on the loading stand, underneath the gold target. Then, the sputterer was placed under vacuum, and the sputtering process began. To guarantee the thorough coating throughout the backbone and the absence of exposed cured PR48, gold was sputtered onto the sample multiple times, each time 90 seconds, obtaining a total coating thickness of approximately 50 nm. Between sputtering procedures, the sample was reoriented to face a different direction. The two long edges of rectangular base, called the bridges, were covered with tin foil in order to keep

the edges nonconductive. This is to conductively isolate the two lattices, which are physically connected by the rectangular base. As a result, when performing the electrodeposition procedure, ions are not able to move through both lattices, separating the anode from the cathode. Due to the complexity of the lattice structure, the center of the backbone was not able to be effectively coated with gold. To deal with this problem, the height of the backbone (and thus the end battery) was reduced by half, to 9 millimeters. This ensured the successful coating of gold throughout the backbone, including the center of the lattice.

Electrodeposition of Lithium Cobalt Oxide (LCO) Cathode

The conductive backbone was placed in a molten KOH solution containing LiOH and CoO at 260 degrees Celsius, obtained from a procedure used by Zhang et al⁵. The solution was required to be heated to 260 degrees in order to melt KOH. Molten KOH was needed to ensure the solubility of cobalt oxide in the solution to form Co^{2+} and O^{2-} . LiOH will be able to dissolve into its respective Li^+ and OH^- ions when mixed with KOH. This allows for both bases to be ionized, producing the necessary ions Li^+ , Co^{2+} , and O^{2-} to yield LiCoO_2 following the electrodeposition. Cobalt was used for the reference electrode, one of the lattice electrodes on the backbone was used for the working electrode, and nickel was used for the counter electrode of the Potentiostat. A cyclic voltammetry experiment was performed for the electrodeposition of LiCoO_2 onto one of the lattices of the conductive backbone. The electrodeposition was done inside a glovebox with argon gas because the electrodeposition cannot be done in the presence of water or water vapor, according to Zhang et al⁵. A major problem faced was that the backbone, which consists of photopolymerized PR48, likely could not withstand the high temperature, leading to the dissolution of the coated gold into the electrodeposition solution. This

phenomenon can be observed in Figure 6, depicting a gold coated PR48 sample before and after being placed in contact with the molten KOH solution. Another hypothesis explaining the dissolution of the coated gold is due to the ineffective adhesion of gold to certain substrates. To fix this problem, another metal must be first coated onto the PR48 surface, serving as an adhesion layer for gold.



“**Figure 6:** Gold-coated PR48 Stick Samples. The two samples are from before (left) and after (right) placement into molten KOH solution.”

Thermal Analysis of Polymer Backbone under LCO Electrodeposition Conditions

The next goal of this project is to explore possible solutions to this problem. The first step was to further strengthen the structural and mechanical properties of PR48 using longer UV post-cure times. PR48 stick samples, shown in Figure 6, were printed using the Ember stereolithography printer. Each sample was post-cured for various amounts of time, ranging from 5 to 60 minutes. Thermal gravimetric analysis (TGA) was used on each sample to determine the effects of cure time on the thermal stability of the sample. TGA is a method that measures the mass of a sample over a period of time as the temperature changes. Each sample was placed into the TGA, where the sample was heated from room temperature to 270 °C at a rate of 10 °C/min,

and then the system was held isothermal for 10 minutes. Results from Table 1 show that cure time had a negligible effect on heat deflection temperature of the sample, since the amount of mass lost for each of the post-cure times experienced a negligible difference in mass loss when the temperature was held at 270 °C.

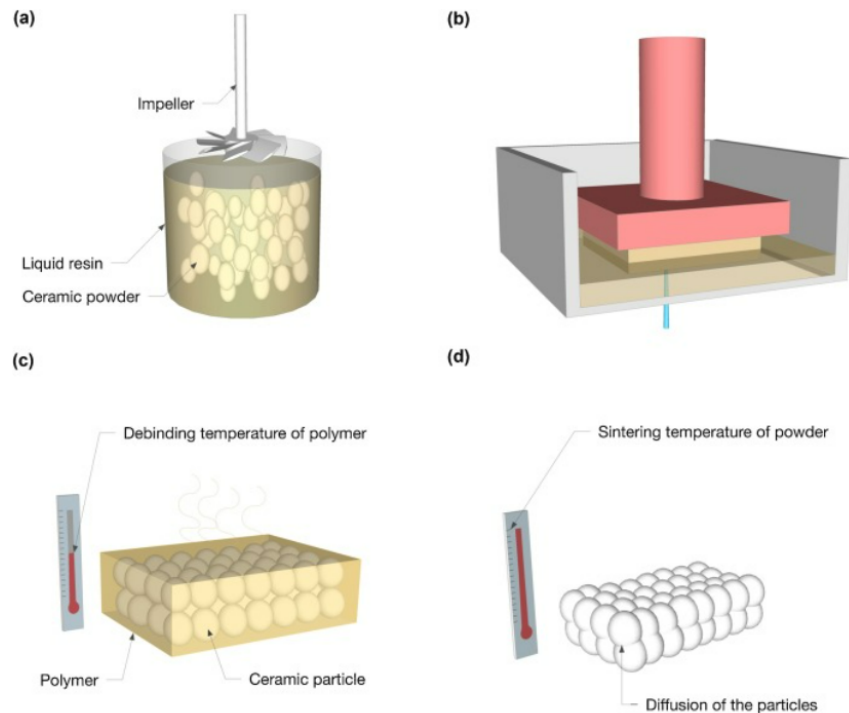
Post-Cure Time	Mass Lost at 270 °C in 10 Minutes (µg)
5	175.80
15	169.66
30	153.04
60	162.21

“Table 1: Relationship Between Post-cure Time and Mass: The table shows the relationship between post-cure time and the mass lost at 270 °C for 10 minutes. Because the changes in mass for each post-cure time only vary on the order of 10 micrograms, it is reasonable to conclude that post-cure time does not have a significant effect on the thermal properties of PR48.

Next, the sputtered gold coating must be considered. Gold, one of the least reactive metals, is unlikely to react with KOH or melt at 260 °C over the course of the 5-minute electrodeposition. Therefore, the most likely possibilities for the vanishing of the gold layer to occur is that gold failed to effectively adhere to the polymer, or there were small pinholes in the sputtered gold coating. As a result, KOH was able to come in contact with the PR48 when placed into the solution. While one solution may be to sputter the gold for longer durations of time, the presence of pinholes suggest that the gold coating is non-uniform. Therefore, a longer sputtering duration may exacerbate the issue with non-uniformity. Another solution is to attempt to implement an adhesion layer before coating the structure with gold. However, metals are also highly thermally conductive, so the PR48 material underneath the metal will still be exposed to the high temperature of the solution. Other methods such as annealing or chemical vapor deposition can ensure an adhesive, uniform, and pinhole-free gold coating, but PR48 would still not be able to withstand the high temperatures of those processes that range around 500 °C.

Exploration of Ceramic Resins

This led to the research of alternative resins that are capable of withstanding a higher temperature of the annealing or chemical vapor deposition process. There have been rapid advances of using ceramic materials for stereolithography within the scientific community in the recent years, due to their high hardness and strength, good temperature performance, excellent thermal shock resistance, and high chemical stability in harsh conditions⁶. A ceramic resin consists of a polymer resin containing a homogenous dispersion of ceramic particles. The printing process is very similar compared to polymers, except it consists of an extra firing step after the print to debind the polymer and sinter the ceramic material, as shown in Figure 7. The firing procedure is commonly associated with ceramic shrinking, so there will need to be a magnification of the CAD design for the structure that is equivalent to the shrinkage percentage.

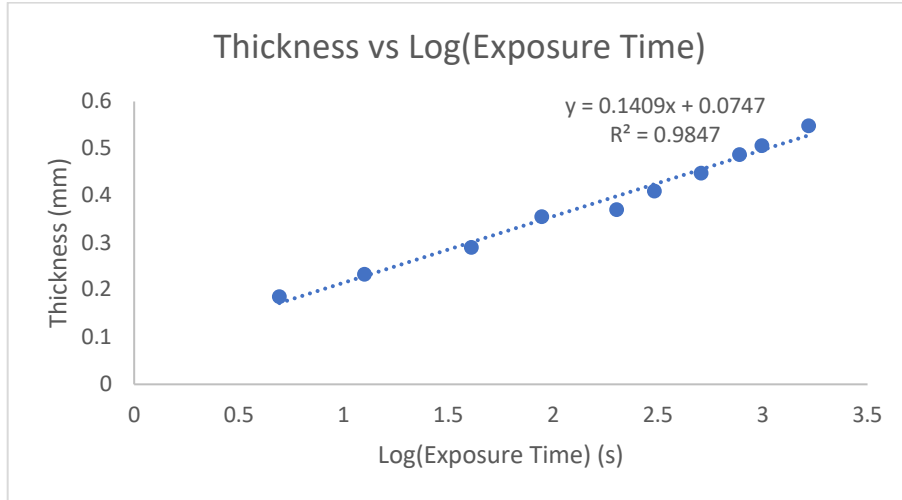


“**Figure 7:** Steps for Additively Manufacturing Ceramic Materials: The steps consist of (a), creating the ceramic resin, (b), printing the structure, (c), debinding the polymer from the ceramic particles, and (d), sintering the ceramic material⁷.”

Using Ceramic Resin for Battery Backbone Structure

Instead of manufacturing a ceramic resin, commercial ceramic resins were explored. After doing research on several commercial ceramic resins, the Formlabs ceramic resin was chosen due to its small print resolution, composition, and suitable polymerization wavelength for the Ember 3D printer. Formlabs ceramic resin consists of homogeneously concentrated silica (SiO_2) nanoparticles in a polymer resin, yielding a silica composed product after firing. This resin will show a 15% shrinkage during firing, so it must be CAD designed to be 115% of its desired size. The firing process consists of a burnout hold for polymer removal, and a sintering hold for the ceramic, requiring a total time of 28 hours. While silica may show brittle behavior and low tensile, it has a high hardness and compressive strength due to its strong ability to withstand vertically applied pressure forces. However, its low reactivity and ability to withstand high temperatures and thermal shock are the most appealing properties that allow it to withstand the high temperature chemical vapor deposition and electrodeposition processes in this project.

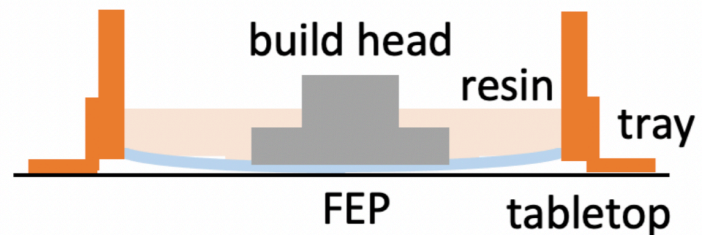
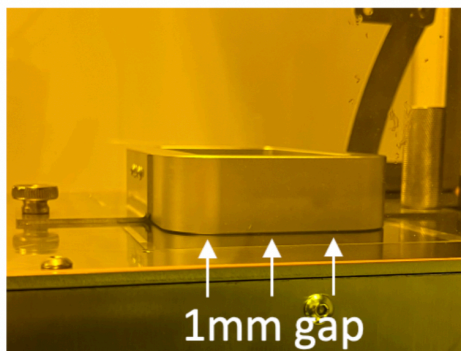
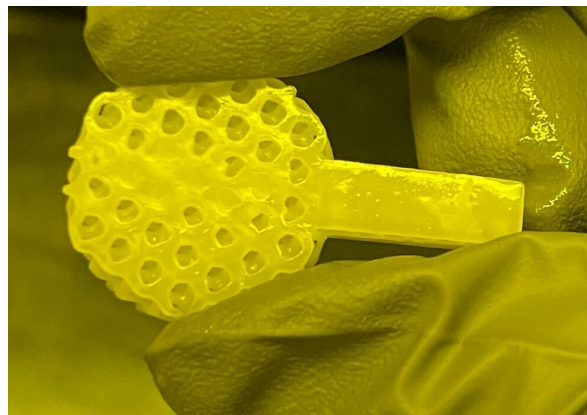
The printing of the ceramic resin will be done on the Titan 3 printer. This printer requires inputs of the PNG files for each layer of the structure to be printed, the cure time of each layer, and the energy dosage of the UV curing light. Due to the novelty of the ceramic resin, an investigation into the correlation between the thickness of the curing layer and the corresponding exposure time was conducted. Thus, the layer-by-layer print thickness for each PNG image can be finely tuned to create the desired printed ceramic structure. Ceramic resin squares were printed with various amounts of cure times, and the corresponding thicknesses of the squares were measured. Taking the log of the exposure time led to a strong linear relationship between the data, as seen in Figure 8. This model can be used to determine cure time for any desired print layer thickness in the hundreds of micron range.



“Figure 8: Relationship Between Cure Time and Layer Thickness: This relationship can be determined for any resin-printer pairing and is crucial for determining the print time for each layer based on the desired layer resolution.”

After attempting to print a ceramic lattice structure with the Titan 3 printer, the final printed layers of the structure were observed to be at a significantly higher resolution than the first several print layers. After troubleshooting, the issue was found to originate from the flexibility of the fluorinated ethylene propylene (FEP) transparent film used in the tray for the printer. The Titan 3 printer was designed such that the FEP film is located 1mm above the glass stage when the tray is fixed into the printer (this is to prevent the FEP film from touching the glass window). Before printing, the build head must be calibrated to ensure that it is in contact with the film before printing the first layer. The calibration of the build head to the home position was done using a method consisting of a piece of paper that is 0.2 mm thick. Thus, before printing, the homed build head pushes the film (located 1 mm above the glass) downwards 0.8 mm since the home position is calibrated to be in contact with the paper, 0.2 mm above the glass. Due to the flexibility of the FEP film, the build head will stay in contact with the film during the print process as the head moves from the z position of 0.2 mm to 0.8 mm. Given that each layer

has a thickness of microns (0.02 mm), 30 layers will be compacted and printed as the “first layer”, since the build head would remain in contact with the film for that distance. This is synonymous to printing the first layer with the sum of the exposure times for the first 30 layers, ultimately compacting the structure around the base. The solution would be to begin the print while the build head is 0.7 mm above the home position. Additionally, sacrificial supports could be added as the print layers for the first 30 layers. Once the structure gets printed, the supports could be removed, as this ensures that there will be no compacting of the layers corresponding to the lattice itself.



“**Figure 9:** Troubleshooting the Overexposed First Layers of the Lattice: The top image depicts the overexposed side of the printed lattice. This side was in contact with the build head, which corresponds to the first layer of the print. The 1mm gap between the FEP film and the transparent UV window was found to be the source of the problem. Based on the way the build head was calibrated, it would bend the film such that there is contact between the two surfaces for the first 30 layers of the print.”

Unfortunately, the electroplating of lithium cobalt oxides onto transition metals remains a highly complex and unexplored area. Due to the difficulty of the electrodeposition of lithium cobalt oxide and the long tuning process for optimizing the printing of the novel ceramic resin, this step of the project was paused due to time constraints. Therefore, the next step in the project, electroplating the lithium anode, was explored.

Electrodeposition of Lithium Anode

Lithium micro-lattices were printed using the Titan 3 printer with sizes varying from 5-10 millimeters in lattice diameter, 0.7 millimeters in beam diameter, and 1 millimeter in space between beams. The curing light of the Titan 3 printer has a greater resolution (25 microns) than the current Ember 3D printer. Thus, the Titan 3 would be able to print the lattice beams with a smaller margin for error.

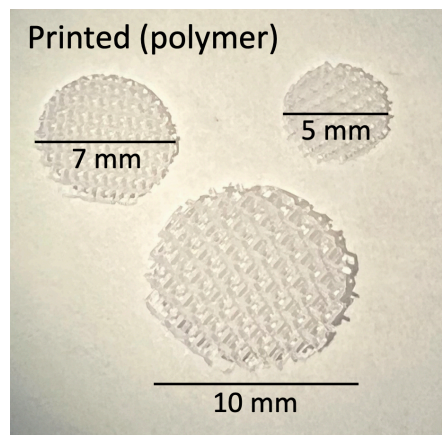


Figure 10: Printed Lithium Micro-lattices: Lattices of varying sizes were printed using the Titan 3 printer to be used for optimizing the electroplating of lithium. Image provided by Yuchun Sun.”

The 10-millimeter diameter singular lattices, as seen in the bottom image of Figure 10, were printed connected to a rectangular handle so that the structure could be held in place during the electrodeposition process. These samples are test structures to be used to optimize

electrodeposition settings for lithium onto the lattice. Once optimized, the electrodeposition settings will be used on the interpenetrating lattices battery backbone. In this process, lithium must be electroplated on a conductive surface, so the printed lattice (made of a cured photo resin containing acrylates) was pyrolyzed. The lattice structures were slowly heated to 1000 degrees Celsius over a duration of 15 hours; this resulted in a pyrolyzed carbon micro lattice capable of conducting electricity and withstanding high temperatures without a change in phase. Pyrolysis resulted in a 74% size reduction of the micro-lattice. This resulted in a lattice diameter of 2.6 mm, lattice thickness of 0.59 mm, and a total length of 4.4 mm. The beam diameter was 0.20 mm, and the spacing between beams was 0.26 mm.

An electrodeposition setup was created with pure lithium serving as the counter electrode, pyrolyzed carbon serving as the working electrode, and a LiTFSI solution serving as the electrolyte. LiTFSI is a common electrolyte found in most commercial lithium-ion batteries due to its high ionic conductivity and chemical/thermal stability. Therefore, it was chosen to serve as an effective solution for the transport of lithium ions in the electrochemical system. The electrodeposition was conducted on a hot plate at 60 degrees Celsius to increase the kinetics of the transport of lithium ions to the working electrode. Additionally, the electrodeposition process was conducted inside a glovebox with argon air due to the reactivity of lithium with oxygen and water. The overall setup can be visualized in Figure 11.

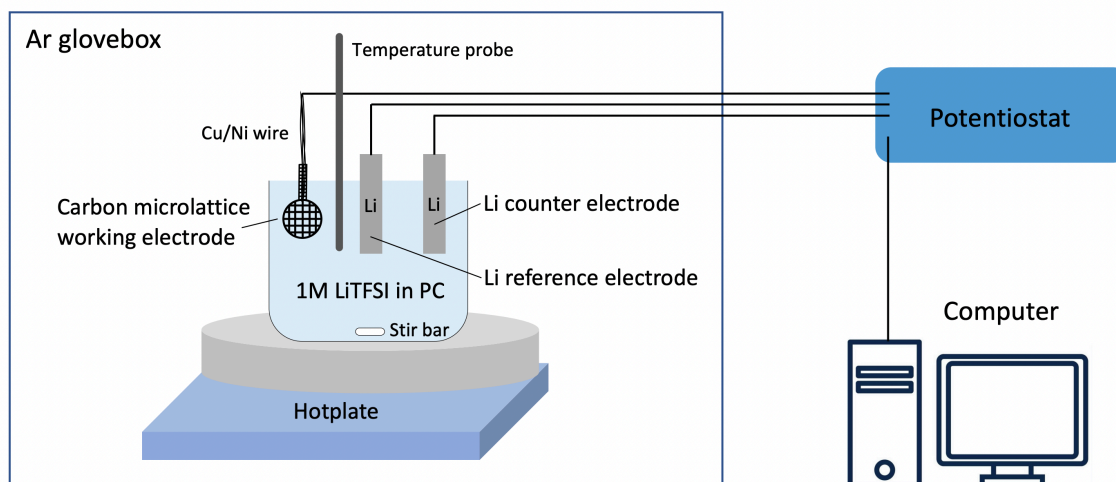
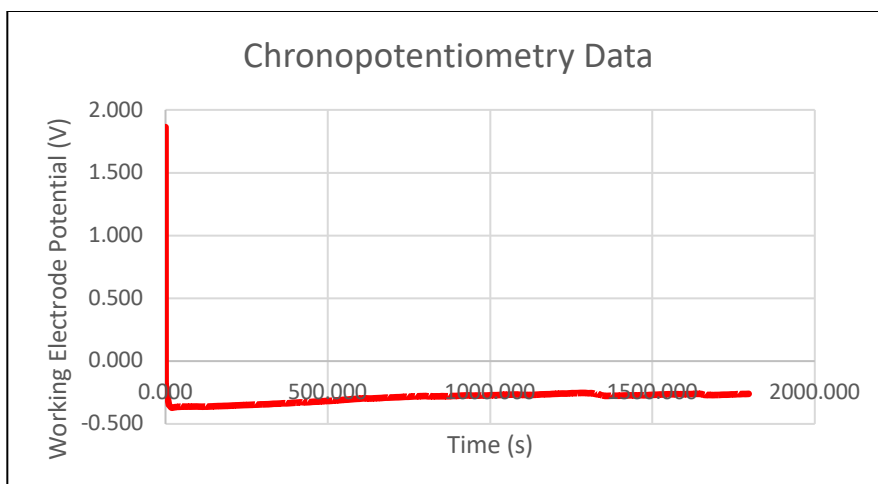


Figure 11: Electrodeposition Setup: The setup for the electrodeposition consists of a lithium counter and reference electrode, the lattice working electrode, the LiTFSI electrolyte, and a potentiostat providing a constant current. Figure provided by Yuchun Sun.”

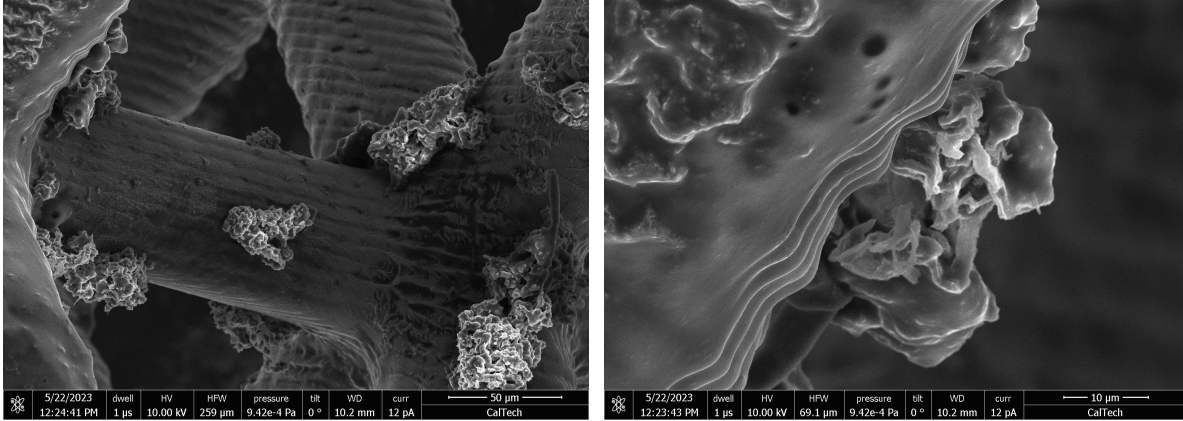
A chronopotentiometry technique was used for the electroplating of Li onto the lattice: this involved the use of a Potentiostat to apply a constant current of 5 mA to the working electrode for a duration of 30 minutes; in response, the working electrode potential varied based on the sample and wire resistance. A chronopotentiometry curve was obtained following the electrodeposition, as observed in Figure 12. The magnitude of the potential was observed to be decreasing over time; since the current was held steady, this implies that resistance of the electrode also decreased over time ($V = I \times R$). This signifies that lithium is being plated onto the gold surface. The addition of lithium, a good conductor, will decrease the resistance of the entire system because conductors allow the free circulation of electrons. Additionally, the resistance of a material is inversely proportional to the cross-sectional area of the material that current is traveling through. This confirms that lithium is being plated onto the lattice beams, since the beam cross sectional area is increasing, thus decreasing the resistance and voltage at the working electrode.



“**Figure 12:** Chronopotentiometry Data for Electroplating: The graph above depicts the change in the working electrode potential over time during the electroplating procedure. This decrease in the magnitude of the working electrode potential at a steady current over time implies a decrease in resistance as more lithium is plated.”

SEM Analysis of Plated Lithium

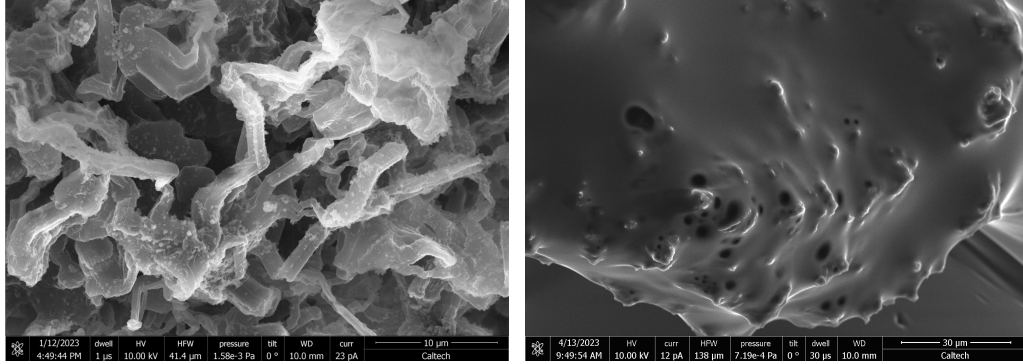
Once the lithium was plated onto the pyrolyzed carbon lattice, the sample was analyzed with a scanning electron microscope (SEM). Dendritic lithium features were observed in sparse regions across the beam surfaces of the pyrolyzed carbon micro-lattice. This may be due to the high nucleation energy barrier required for lithium to be deposited onto a carbon surface. As a result, lithium would only nucleate onto the carbon lattices in small areas. This is far from the desired uniform lithium layer that entirely covers all lattice beams of the structure. Additionally, any further lithium nucleation would be on the small amounts of lithium already nucleated, instead of on the carbon lattice surface. This results in the formation of clumps, and long, needle-like or dendritic lithium features that do not fully cover the pyrolyzed carbon lattice. These features can be observed in Figure 13.



“Figure 13: SEM Images of Dendritic Lithium Growth: The images above depict dendritic growth of lithium on the pyrolyzed carbon surface when a direct current was applied for 15 minutes.

Addition of a Titanium and Gold Layer to Pyrolyzed Carbon Micro-lattice

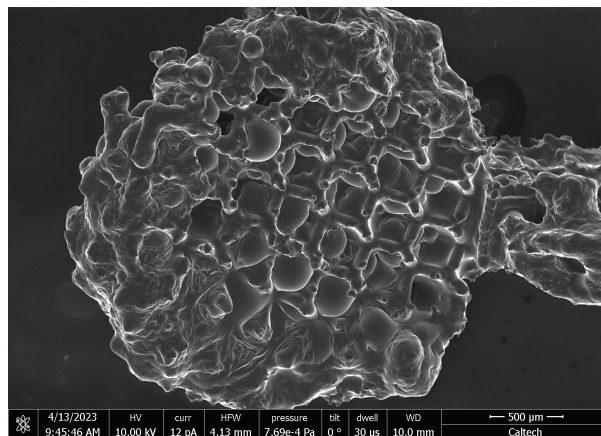
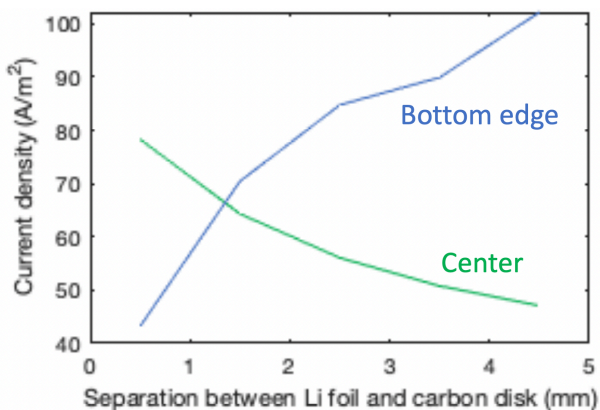
This issue could be fixed by coating the pyrolyzed carbon lattice with titanium then gold. Yan et. al suggests that the nucleation energy barrier for lithium to be deposited onto a gold surface is significantly lower⁸, so we can expect significantly more uniform growth of lithium on gold in the electrodeposition process. A thin layer of titanium was first sputter-coated onto the pyrolyzed carbon micro-lattice, serving as an adhesion layer for the gold coating; this is necessary because of gold’s low chemical reactivity, leading to its poor adhesion on the carbon surface¹⁰. This was proceeded with gold being sputter-coated onto the sample. The sample underwent a 30-minute electroplating process. This was compared with a 30-minute electroplating process on a sample without the Ti/Au layer. The SEM images of both samples in Figure 14 show that having the titanium and gold layer yields a significantly more uniform lithium coating. This proves that using a metal that has a lower nucleation energy barrier with lithium will yield a more uniform electrodeposited lithium surface.



“**Figure 14:** SEM Images of Electroplated Lithium on Pyrolyzed Carbon vs Gold: Lithium was deposited on pyrolyzed carbon (left) and on gold (right) for a 30 minute duration.”

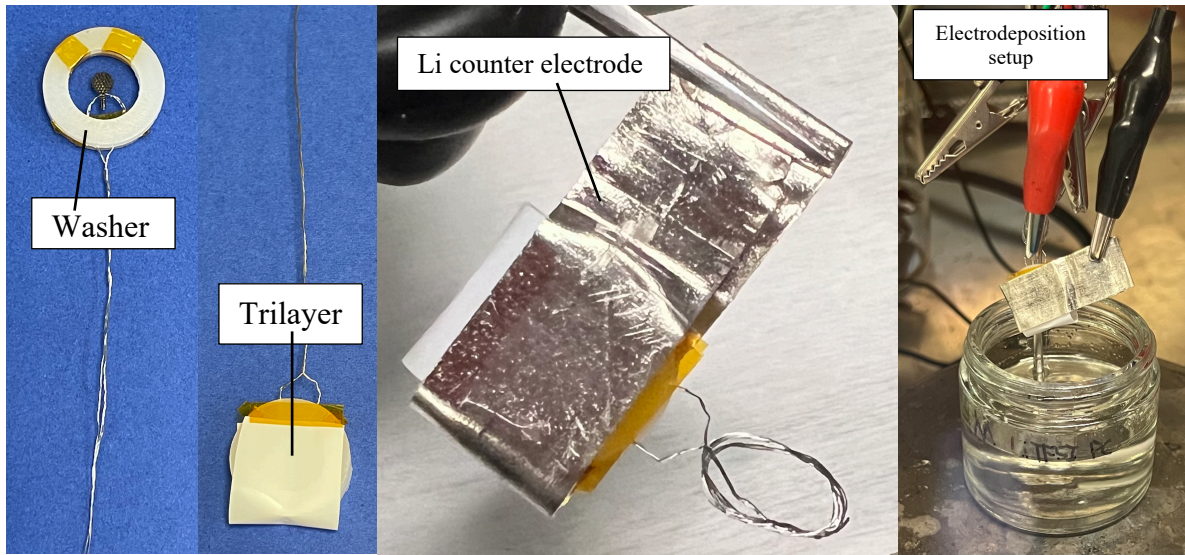
Lithium Electrochemistry Setup Optimization

Another problem encountered during the electroplating process was the orientation and placement of the counter electrode relative to the working electrode. This had a significant effect on the location of the plated lithium on the micro-lattice. The side of the micro-lattice facing the lithium counter electrode received significantly more lithium plating than the side facing away from the lithium counter electrode. Additionally, when the counter electrode was placed further away from the micro-lattice, the plated lithium was discovered to be more concentrated at the edges of the lattice. A COMSOL simulation of the electroplating procedure was conducted by mentor Yuchun Sun, which demonstrated that when the separation between the working and counter electrodes increases, the current density at the lattice’s center decreases, while the current density at the lattice’s bottom edge increases. As a result, the plated lithium was discovered to be more concentrated around the lattice’s bottom edge.

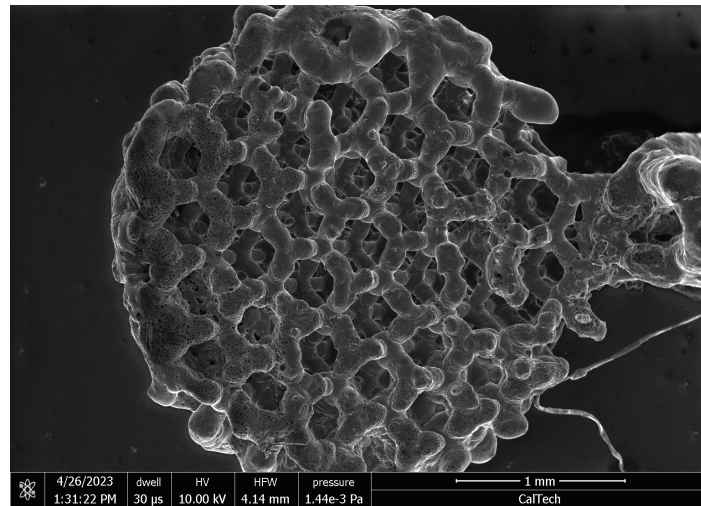


“**Figure 15:** Relationship Between Current Density and Electrode Separation: The graph (right) demonstrates that there is an optimal separation between the lithium counter electrode and the working electrode, such that the current density is uniform throughout the entire sample. Provided by Yuchun Sun, based on COMSOL simulation. The SEM image on the left depicts lithium coating highly concentrated around the bottom edge of the sample.”

Due to these issues, a device for holding both electrodes in place to effectively control their separation distance was manufactured. The counter electrode was folded around the device holding the working electrode so that both sides of the micro-lattice are facing the counter electrode. The device consists of 2 high density polyethylene washers, 2mm in thickness, holding the sample in place in the middle. This washer will maintain the separation distance between the working and counter electrodes at approximately 1.7 millimeters. This was calculated subtracting half of the thickness of the micro-lattice from the thickness of the washer. A copper/nickel wire, 130 microns in diameter, was bound to the micro-lattice and the washers; this conductive wire will be connected to the working electrode. Lastly, a porous polyethylene polypropylene trilayer was wrapped around the washers, followed by the lithium counter electrode. This was done to prevent physical contact between the counter electrode and the working electrode, while still allowing fluids to flow through the material. The new electrodeposition setup was incorporated, reducing the clumping of lithium around the edges of the lattice, as seen in Figure 16.



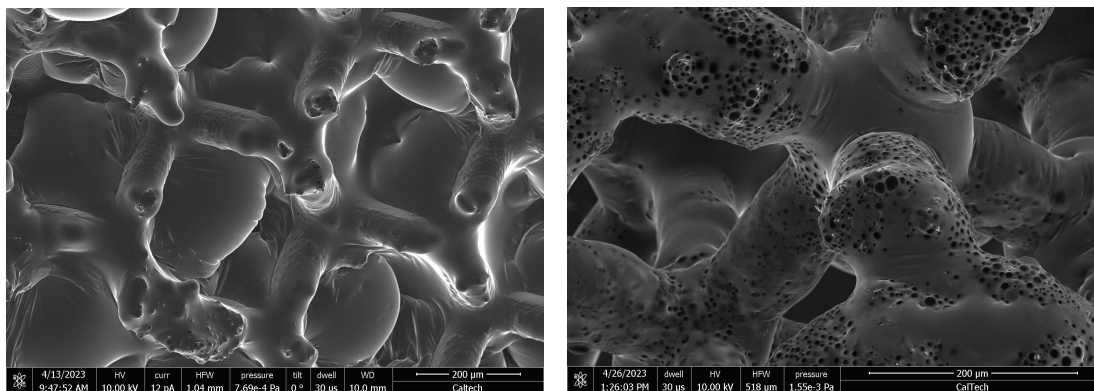
“**Figure 16:** Fabrication Process of New Electrodeposition Setup: The copper wire that is threaded within the lattice is sandwiched between two washers. The trilayer is wrapped around the washer, and the counter electrode is wrapped around the trilayer. The electrode clamps are attached to their respective electrodes, and the setup is placed into the electrolyte on a hot plate.”



“**Figure 17:** SEM Image of Entire Micro-lattice with New Electrodeposition Setup: The new setup has significantly reduced the separation distance from around 10-15 mm to 1.7 mm. As a result, the clumping of lithium around the edges of the lattice has significantly decreased but is still present. This is because the 1.7 mm separation is still larger than the optimal separation of around 1.3 mm, so the presence of clumping is still expected.”

However, the electroplating duration was clearly too long because the SEM images of the sample also showed that the micro-lattice beams were not as well defined due to the large layers of lithium that were covering them. This also proves that some areas of the lithium coating were

thicker than others. Shortening the time of electrodeposition may still yield the uniform deposition of lithium on gold yet it may also prevent certain areas of the beam from receiving too much electroplated lithium and become thicker than other areas. Therefore, the effects of the time of electrodeposition on the coating morphology was investigated. Three electrodepositions were conducted on three identical Ti/Au coated micro-lattices; the durations of the electrodepositions were 30 minutes, 15 minutes, and 10 minutes, respectively. It was observed that both the 15- and 10-minute electrodepositions had a visibly thinner coating on the beams compared to the 30-minute electrodeposition. Additionally, as seen in the SEM images in Figure 18, the 30-minute electrodeposition led to lithium covering a significant amount of space between the lattice beams, blocking the ability to see the beams underneath the top surface. This was not the case for the two shorter electrodepositions.



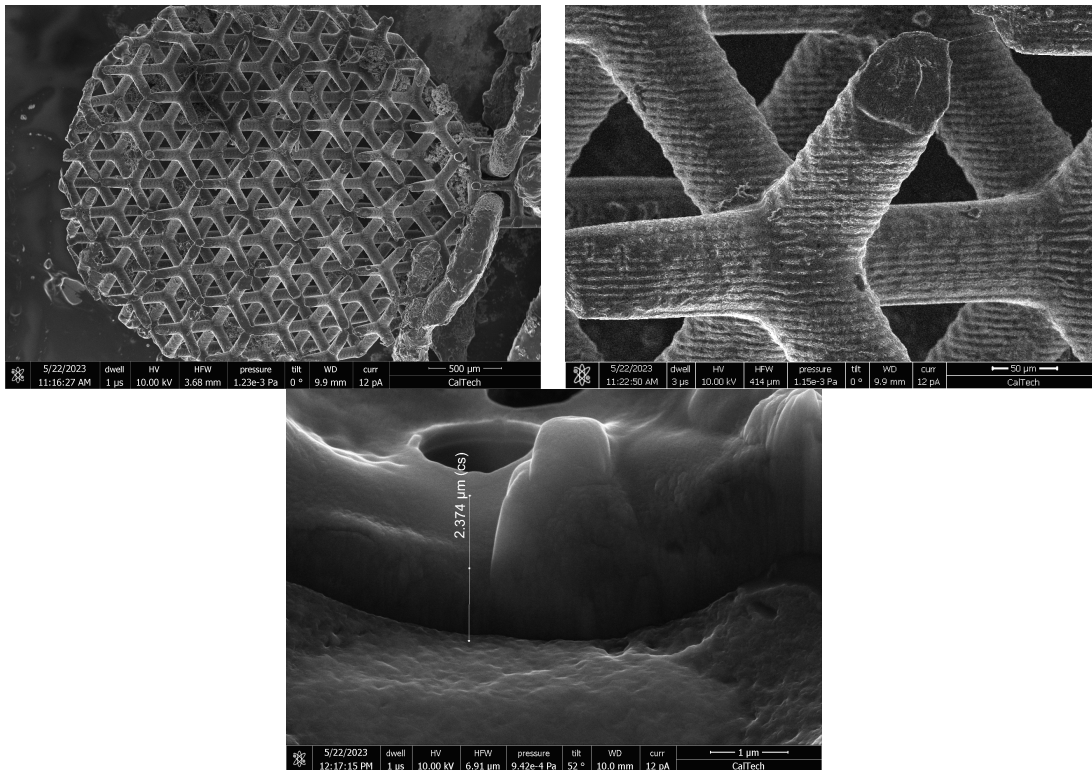
“Figure 18: SEM Image of Electrodeposited Lithium at Various Durations: Lithium was deposited on gold for a 30-minute duration (left), 15-minute duration (right).”

It is also noteworthy to observe the difference between the 15-minute and 30-minute plating. Black spots approximately 1-2 microns in diameter were observed in the 15 minute-coating as well as the 30-minute coating, but to a significantly less extent. These black spots were analyzed using energy-dispersive x-ray spectroscopy and were discovered to be holes on the surface of the coating, instead of a foreign material. Eventually, these holes will be either

filled or covered by the additional lithium coating as the duration of the electrodeposition increases. However, the underlying cause of the formation of these holes remains obscure but may be attributed to the implementation of a direct current in the electrodeposition. While a longer electroplating time may lead to the covering of the holes, there is the clear tradeoff of having an excess of lithium coating that fills the space between the beams, with some coated areas thicker than others, ultimately distorting the lattice structure.

Utilization of Pulse Current in Lithium Electrodeposition

The effects of utilizing a pulse current in contrast to the conventional direct current was also investigated in effort to solve the electrodeposition duration tradeoff from using a direct current. A pulse current, where the current is cycled on and off at steady time intervals, could potentially better control the properties of the electroplated lithium layers. Due to the relatively low nucleation energy barrier for lithium to be deposited onto gold, a pulse current could potentially offer a more uniform coating of lithium on the lattice. Additionally, sources suggest that employing a pulse current can significantly reduce the internal stress, minimize porosity, and increase material strength compared to DC⁹. Therefore, a chronopotentiometry technique, consisting of a 5-mA current for 1 second with a 1 second delay over 60 minutes was chosen and utilized with the same electrodeposition setup. SEM images of the lithium coated sample is shown in Figure 19. The most noticeable observation entails a reduction of visible holes in the below SEM images, compared to the SEM images of the structures exposed to a direct current. However, the presence of holes persists, as seen in the bottom image of Figure 17, with an unknown underlying cause. Additional electrochemical analysis could be conducted to minimize the number or dimensions of these holes.



“**Figure 19:** SEM Images of Sample Following 60-minute Pulse Current: SEM images depict a uniform coating throughout the majority of the micro-lattice. The lines that appear on the beams (top right) represent each layer of the 3-D printed lattice structure. There seems to be very few holes in the SEM images. The thickness of the plated lithium was found to be around 2-3 microns.”

Based on the SEM images shown in Figure 15, the 60-minute pulse current chronopotentiometry technique has proven to be the most effective in yielding a smooth, uniform lithium coating. There still remains some sparse clusters of concentrated lithium plating around the edges of the lattice, suggesting that the working and counter electrode separation should be further decreased. However, the pulse current does reduce the buildup of lithium coating around the edges of the lattice compared to a direct current of half the total electrodeposition time (the duration of the pulse current must be compared with the half of the duration of the constant current). This suggests that the rate of lithium electrodeposition is higher when the working electrode is subject to a constant current density, compared to a pulsed current density of the same magnitude. A focused ion beam was used to etch a portion of the plated lithium on a beam

of the micro-lattice, and an SEM image was taken of the cross section. The thickness of the lithium coating was then measured to be approximately 2.4 microns.

Having solved the challenges of ion transport, current density distribution, and plating thickness, the micro-lattice will be scaled up to larger sizes and more electroplating will be tested. The optimal current density for even lithium plating across larger micro-lattices must be determined. Additionally, the next step of this project is to determine the thickness of the electroplated lithium as a function of time in which the pulse current is applied.

Electroplating the anode provided unique insight for techniques to consider when electroplating lithium cobalt oxide for the cathode. The micro-lattices used to test the lithium electrodeposition, when pyrolyzed, became extremely stable at high temperatures. Unfortunately, the original interpenetrating lattices structure cannot undergo pyrolysis because the entire structure will become conductive, and thus lithium cobalt oxide and lithium cannot be selectively electrodeposited onto each lattice. However, pyrolysis may be necessary to provide the increased thermal and chemical stability of the structure when electrodepositing LCO in the molten KOH solution. Therefore, the proposed interpenetrating lattices structure may not serve as a feasible design for the backbone of the 3-dimensional battery manufacturing process.

Alternatively, designing two physically separated 3-dimensional structures that can be later combined after electrodepositing LCO and lithium may prove to be a significantly easier process. This way, both electrodes are kept separate and both electrode backbone structures, when printed, can be pyrolyzed. Additionally, creating two separate electrode backbone structures allows for other methods of LCO plating to be explored, since the electrodeposition of LCO is extremely complex.

CONCLUSION

Summary

3-D lithium-ion batteries show a lot of promise in future studies because it breaks the tradeoff between achievable energy density and power density in the standard commercial 2-D lithium-ion battery. Due to the difficulty in manufacturing current proposed 3-D battery structures, this thesis proposes the development of an alternative 3-D battery structure, comprising of two interpenetrating lattices that will serve as the electrodes, one that could be created using additive manufacturing. Additive manufacturing has shown extraordinary capabilities for controlling tuning the architectures of desired structures with high precision; its techniques continue to be improved with increased resolution and wider ranges of materials able to be utilized. For these reasons, additive manufacturing proves to be a promising technology for the efficient development of more capable lithium-ion batteries in the future. Therefore, this thesis explores the feasibility of manufacturing a 3-D lithium-ion battery by using additive manufacturing coupled with electrochemistry.

The battery backbone was printed using the Ember 3-D stereolithography printer. A 15-minute UV post-cure was used to strengthen the mechanical properties of the backbone. After covering the bridge in tin foil, gold was sputtered onto the lattices to give them conductive properties, but making sure they were not conductively connected. This is to make sure current can only run through one lattice at a time, allowing for selective electrodeposition of the lithium anode on one lattice and the lithium cobalt oxide cathode on the other lattice. The electrodeposition of lithium cobalt oxide was unsuccessful due to the harsh conditions of the electrolyte, consisting mainly of molten potassium hydroxide, a strong base, at 260 °C. Thermal gravimetric analysis proves that the structural and mechanical properties of PR48 could not be

non-negligibly strengthened with any duration of UV post-curing. The likely presence of pinholes in the sputtered gold coating requires high temperature annealing or chemical vapor deposition, leading to the exploration of alternative resins such as ceramic resin that are high-temperature withstanding. Due to the long process of tuning print parameters for novel resins and the difficulty of the LCO electrodeposition, this step of the project was paused due to time constraints. The electrodeposition of lithium on a test micro-lattice proved successful, yielding a uniform 2.5-micron lithium coating throughout the entire structure. The successful coating is attributed to the utilization of a 1 second on, 1 second off pulse current for 60 minutes, in addition to establishing an electrodeposition setup consisting of the lithium counter electrode surrounding the lattice with 1.7 mm separation. Shortening the electrode separation from 1.7 to 1.3 mm may further eliminate the small clumping of lithium around the edges of the lattice. The successful manufacturing of 3-D battery backbone and the electroplating of the lithium anode onto the beams demonstrates tremendous potential for utilizing additive manufacturing coupled with electrochemistry for the aiding the design and assembly of next generation 3-D lithium-ion batteries.

Future Work

Although additive manufacturing presents an efficient and effective way of manufacturing 3-D lithium-ion battery architectures, there remains significant improvements to be made before they can be tested, starting with the plating of lithium cobalt oxide around the lattice beams. The successful electrodeposition of lithium suggests that pyrolysis allows for the lattice structure to be thermally stable for the annealing or chemical vapor deposition of gold. However, pyrolysis will result in the entire interpenetrating lattices structure to become

conductive, eliminating the possibility of selectively electrodepositing lithium on one lattice and lithium cobalt oxide on the other. Therefore, it may be necessary to explore alternative structures where the electrodes are kept separate until they are plated with their respective anode and cathode materials. This allows for more flexibility on how lithium cobalt oxide can be plated. Once this is done, the separate structures can be bound together or even kept separate within the battery depending on the architecture of the electrodes.

Alternatively, the current interpenetrating lattices structure may still be utilized if it is coated with a titanium adhesion layer before gold is sputtered on. While this could result in a significantly more uniform gold coating, the presence of any pinhole could still result in the damage of the PR48 underneath the metal layers. Additionally, the high temperature of the electrodeposition solution may still likely alter the physical structure of the PR48 underneath the gold and titanium layers. It is unknown if nanoscale pinholes were present in the lithium plated micro-lattices even though none were detected with SEM. However, using the titanium adhesion layer may still be worth attempting before moving on to explore alternative 3-D battery structures. The best way to move forward entails further optimization of the parameters for printing the ceramic resin. This will solve the main issue of the thermal stability of PR48 in the high temperature electrodeposition solution. After successfully printing a ceramic resin lattice at the desired resolution, the titanium adhesion layer and gold will then be coated. Once lithium cobalt oxide is successfully plated, LiTSFI electrolyte may be added to the battery cell to test its performance. Most importantly, when the optimal lithium cobalt oxide electrodeposition technique is discovered, the additive manufacturing and electrochemistry method can be utilized to create 3-D lithium-ion batteries from many complex 3-D architectures. This is the key to improving the energy density of today's battery technology.

References

1. Ren, Guorui, et al. *Applied Energy* 204, 47–65 (2017).
2. J. W. Long, B. Dunn, D. R. Rolison, and H. S. White. *Chemical Reviews* 104 (10), 4463-4492 (2004).
3. P. Sun, X. Li, J. Shao, and P. V. Braun. *Advanced Materials* 33 (1), 2006229 (2021).
4. Hung, Chih-Hsuan, Srikanth Allu, and Corie L. Cobb. *Journal of the Electrochemical Society* 168 (10), 100512 (2021).
5. K. Narita, M. A. Citrin, H. Yang, X. Xia, and J. R. Greer. *Advanced Energy Materials*, 11 (5), 2002637 (2021).
6. H. Zhang, et al. *Science Advances* 3 (5), 1602427 (2017).
7. S. Zakeri, M. Vippola, and E. Levanen. *Additive Manufacturing* 35, 101177 (2020).
8. Yan, Kai, et al. *Nature Energy* 1 (3), 16010 (2016).
9. Todeschini, Matteo, et al. *ACS Applied Materials & Interfaces* 9 (42), 37374–37385 (2017).